# Spatial-Spectral Mapping Beamspace MIMO Receiver Enabled by a Programmable Space-Time-Modulated Metamaterial Antenna

Shaghayegh Vosoughitabar<sup>#</sup>, Alireza Nooraiepour<sup>\*</sup>, Waheed Bajwa<sup>#</sup>, Narayan Mandayam<sup>#</sup>, Chung-Tse Michael Wu<sup>#</sup>

\*Department of Electrical and Computer Engineering, Rutgers University, USA

\*Qualcomm Inc., USA

ctm.wu@rutgers.edu

Abstract - This paper leverages a space-time-modulated metamaterial (ST-MTM) antenna as a beamspace multiple-input multiple-output (MIMO) receiver, which facilitates the retrieval of information from multiple users transmitting distinct data on the same carrier frequency. In this scenario, the information received from each user, located in a specific direction, is mapped to a distinct harmonic frequency component within the received spectrum. The phase constant  $(\beta)$  of each tunable composite right/left-handed (CRLH) unit cell in a leaky wave antenna (LWA) is periodically modulated in the time domain, generating harmonic frequencies around the carrier frequency of the received signal. By applying a proper time-modulated sequence to each unit cell, the power levels of the harmonics, extracted from one port of the receiver, reach their maximum values at different directions, enabling spatial-spectral mapping. The measured bit-error-rate (BER) results, obtained using a fabricated prototype as the receiver, confirm the successful retrieval of data concurrently sent by multiple users.

Keywords — metamaterial, multiple-input multiple-output (MIMO), receiver, space-time-modulated structure, time-modulation.

### I. Introduction

Modern wireless communication services demand mobility, capacity, reliability, and spectral efficiency. In this context, designing high-performance and intelligent antennas, capable of operating in both transmission and reception modes, is crucial to meet these demands [1]. In recent years, solutions have been developed to send and receive signals accurately and efficiently, involving work across spatial, frequency, and temporal domains. To this end, the concept of beamspace multiple-input multiple-output (MIMO) communication, which multiplexes data across orthogonal spatial beams, is proposed to achieve near-optimal performance [2]. Nevertheless, utilizing lens antennas for the beamforming network still necessitates a complex I/O interface, involving the use of multiple RF ports.

On the other hand, time-modulated arrays (TMAs) manipulate the radiation pattern of antenna arrays by periodically connecting and disconnecting the antenna elements to and from the feeding network, which can realize an ultra-low side lobe level within the array's fundamental frequency pattern [3]. Moreover, the harmonics produced by TMAs can be used in versatile applications for wireless communications and radar systems [1], [4]–[8]. For example, TMAs are effectively employed as receivers, harnessing their

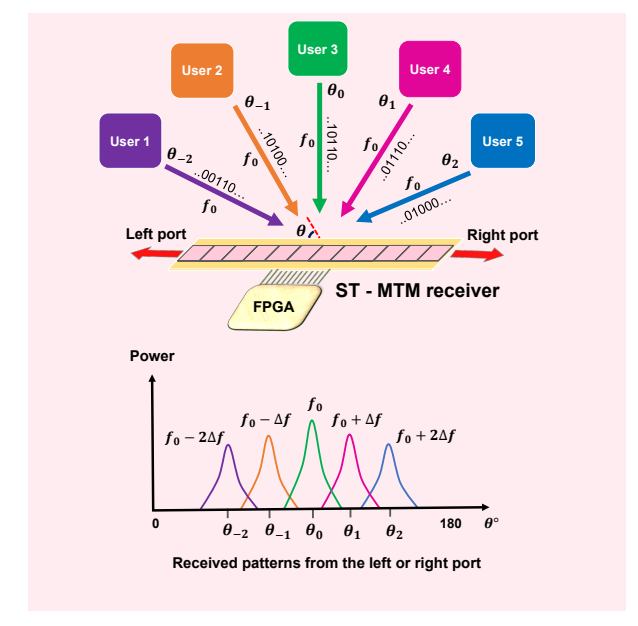


Fig. 1. Spatial-spectral mapping through ST-MTM receiving antenna for multiuser beamspace MIMO communication.

harmonic beam scanning capabilities [9], [10]. However, traditional TMAs, which incorporate phased arrays with switches, might suffer from reduced radiation efficiency during times when antenna elements are inactive.

In contrast, metamaterial antennas provide advantages in terms of simplicity and adaptability over conventional phased arrays [11], [12]. A recent innovation involves a space-time-modulated metamaterial (ST-MTM) leaky wave antenna (LWA) with digitally programmable composite right/left-handed (CRLH) unit cells [13], which facilitates harmonic beam scanning and allows for nonreciprocal transmission and reception of signals. In this work, we employ the programmable ST-MTM LWA as a beamspace MIMO receiver, enabling the simultaneous retrieval of information transmitted by multiple users at different angles by leveraging the spatial-spectral mapping relationship of the generated harmonic components, as depicted in Fig. 1.

# II. PROGRAMMABLE SPACE-TIME-MODULATED METAMATERIAL ANTENNA RECEIVER

By incorporating varactor diodes in a CRLH unit cell, consisting of an interdigital capacitor and a shunt-stub

inductor, a tunable metamaterial unit cell is achieve Changing the varactors' bias voltages allows the constant  $(\beta)$  of the unit cell to toggle between  $\beta$  and negative values at a specific frequency in its far region. Therefore, a digitally programmable LWA is by cascading several tunable CRLH cells. In this archi periodically changing the  $\beta$  of each unit cell in the domain, with a modulation frequency of  $\Delta f$ , resharmonic generation [13]. It is noted that in this each unit cell is always radiating, unlike the convex TMAs where some antenna elements are inactive dur off-periods of the switches.

Here, we consider the ST-MTM LWA as a receiver scenario, a signal with frequency  $f_0$  coming from an is captured by the CRLH cells, and harmonics are ge inside the LWA, which can be received from either of the antenna's two ports. The received signal from the right port of the architecture shown in Fig. 2 can be written as [13]:

$$R(\theta, t) = S(t) \sum_{n=1}^{N} e^{-\alpha(n-1)p} e^{jk_0(n-1)p\cos\theta} U_n(t), \quad (1)$$

where in one period we have:

$$U_n(t) = \sum_{u=1}^{L} \gamma_n^u H_u(t), \tag{2}$$

$$H_u(t) = \begin{cases} 1 & \frac{(u-1)T}{L} \le t \le \frac{uT}{L} \\ 0 & \text{Otherwise.} \end{cases}$$
 (3)

Moreover,  $\gamma_n^u$  is as follows:

$$\begin{split} \gamma_n^u &= \prod_{i=1}^n e^{-j\varphi_i^u},\\ \varphi_i^u &= \begin{cases} \beta_0 p, & \mathbf{q}_i^u = 0 \quad \text{(State 0)} \\ \beta_1 p, & \mathbf{q}_i^u = 1 \quad \text{(State 1)} \end{cases} \text{ in } \frac{(u-1)T}{L} \leq t \leq \frac{T}{L}. \end{split} \tag{4}$$

The incoming signal S(t) has a frequency of  $f_0$ , N represents the number of CRLH cells in the leaky wave antenna, p denotes the length of each unit cell,  $\alpha$  is the leakage factor, and L stands for the sequence length in one period  $(T=1/\Delta f)$ . Also,  $\mathbf{q}_i^u$  represents the state of the  $n^{th}$  unit cell in  $u^{th}$  time interval. Furthermore,  $k_0=2\pi f_0/c$  denotes the propagation constant of the incoming signal, where c is the speed of light. Since  $U_n(t)$  is a periodic function, it can be expanded in the form of Fourier series. After obtaining the Fourier coefficients and substituting the series into (1), we have:

$$R(\theta, t) = \sum_{\nu = -\infty}^{\infty} e^{j2\pi(f_0 + \nu \Delta f)t} M(t, \nu, L, \theta),$$
 (5)

where

$$\begin{split} M(t,\nu,L,\theta) &= \\ \operatorname{sinc}(\frac{\pi\nu}{L}) e^{\frac{j\pi\nu}{L}} \sum_{u=1}^{L} e^{\frac{-j2\pi\nu u}{L}} \sum_{n=1}^{N} \frac{\gamma_{n}^{u}}{L} e^{-\alpha(n-1)p} e^{jk_{0}(n-1)p\cos\theta} \,. \end{split} \tag{6}$$

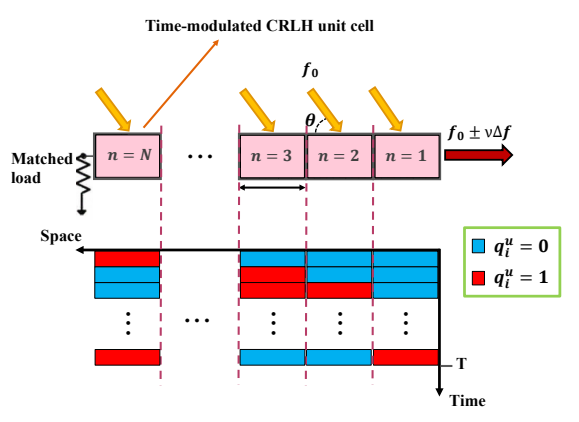


Fig. 2. ST-MTM receiving antenna.

As evident, the spectrum of the received signal includes an infinite number of harmonics around  $f_0$ .

Fig. 3(a) demonstrates the designed tunable CRLH unit cell with the corresponding equivalent circuit model, while its dispersion diagrams for two bias voltages of the varactors are shown in Fig. 3(b). As observed, adjusting the bias voltage results in changes to  $C_{var}$ , consequently causing a shift in the dispersion diagram. It is noted that around 2.1 GHz,  $\beta$  is negative under "Bias 0" condition, while becomes positive when "Bias 1" is applied to the varactors. Considering these two binary states as state 0 and state 1, one can design a space-time-modulated CRLH antenna by applying periodic sequences to the cells of the architecture.

As illustrated in Fig. 1, let us assume an incoming signal with  $f_0$  frequency is radiated to the ST-MTM antenna from the  $\theta$  angle (0° <  $\theta$  < 180°), and the fundamental and harmonic power levels, extracted from one of the antenna ports, resemble the patterns shown in Fig. 1. In this case, the signal with  $f_0$  frequency coming from  $\theta_{\nu}$  angle, can be extracted from  $f_0 + \nu \Delta f$  at this port, since most of the incoming signal power is converted to this frequency component and other generated harmonics are negligible. It is noted that the key element in spatial-spectral mapping is creating this cross beam isolation. In this case, the receiving antenna can retrieve the information of multiple users located in different directions, all sending signals with the same carrier frequency at the same time, by examining different harmonic components.

# III. EXPERIMENTAL VERIFICATION

A prototype with 9 tunable CRLH cells is fabricated on a RO5870 substrate with a dielectric constant of 2.33 and thickness of 1.57 mm to investigate the spatial-spectral mapping functionality. The incorporated varactors are SMV2019 from Skyworks and the desired positive and negative phase constants can be achieved by applying bias voltages of 0.1 V and 3 V to the varactors, respectively.

Fig. 4(a) indicates the measured fundamental and harmonic patterns by applying the periodic sequence illustrated in Fig. 4(b) with  $\Delta f=3.7$  MHz to the cells through an FPGA. The patterns are attained by emitting a signal with  $f_0=2.12$ 

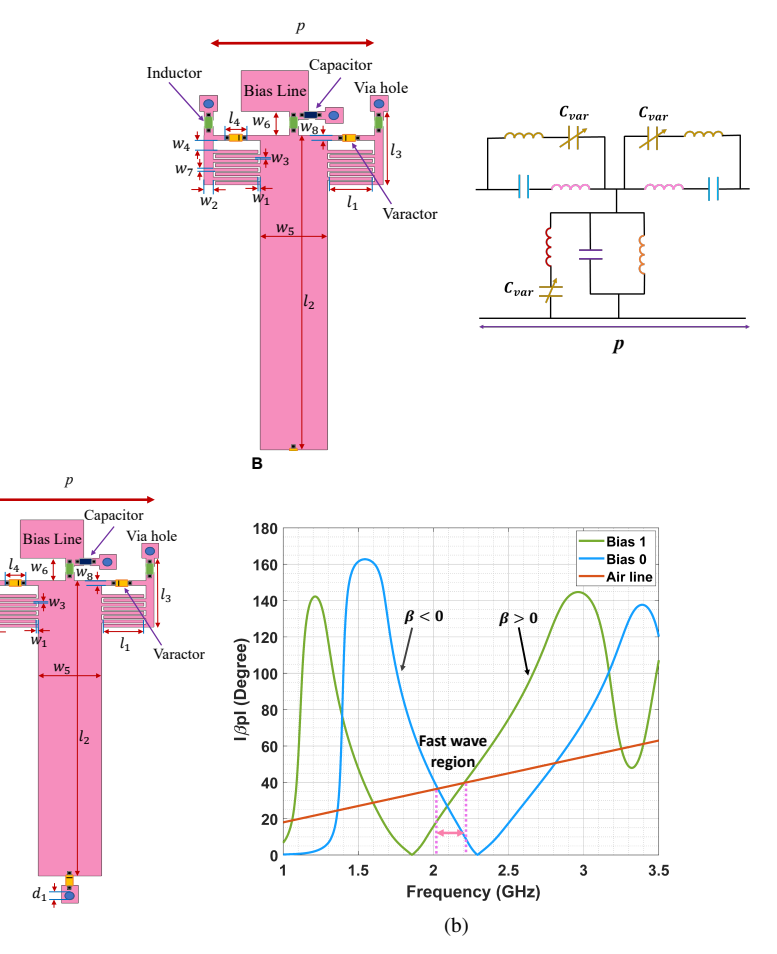


Fig. 3. (a) Tunable CRLH unit cell schematic and its simplified equivalent circuit model. The dimensions (millimeters) are:  $w_1=0.2, w_2=0.8, w_3=0.15, w_4:$  31.5,  $l_3=$  bigs voltage

 $31.5, l_3 =$  bias voltag pF in Bias



Fig. 4. (a) Normalized received patterns of the measured fundamental and first harmonic frequencies in dB, extracted from the right port, after radiating a signal from  $\theta$  angle to the prototype, where  $N=9,\ f_0=2.12$  GHz,  $\Delta f=3.7$  MHz,  $\beta_0 p=-24^\circ,\ \beta_1 p=30^\circ;$  (b) Corresponding sequence in one period.

GHz from different angles and recording the fundamental and harmonic levels from the right port. The calculated patterns are also provided for comparison by taking  $\beta_0 p = -24^\circ$ ,  $\beta_1 p = 30^\circ$ , according to the dispersion diagram of the unit

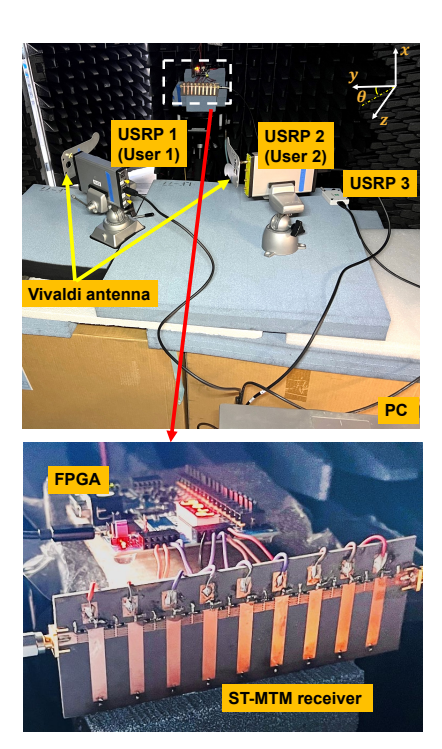


Fig. 5. BER measurement setup.

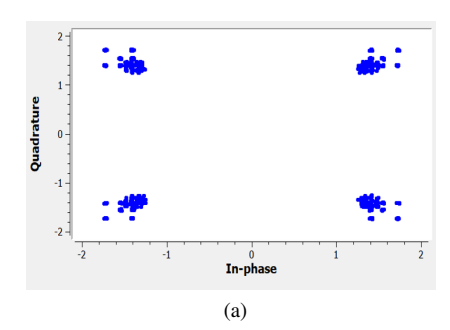
cell depicted in Fig. 3b. As can be seen, if User 1 is located in a direction where  $40^{\circ} < \theta < 60^{\circ}$  and User 2 is positioned in an angle where  $115^{\circ} < \theta < 140^{\circ}$ , more than 10 dB isolation is achieved between  $f_0 - \Delta f$  and  $f_0 + \Delta f$  harmonic components at the right port. In this case, it is expected that the information of User 1 and User 2 can be extracted from  $f_0 - \Delta f$  and  $f_0 + \Delta f$ , respectively.

A measurement setup is designed to investigate the retrieval of data, sent by two users, which are positioned at  $\theta =$  $45^{\circ}$ ,  $\theta = 125^{\circ}$ , as shown in Fig. 5. In this setup, IEEE 802.11p standard [15] is implemented for transmitting and receiving Orthogonal Frequency Division Multiplexing (OFDM) packets with uncoded QPSK modulation through employing GNU Radio software and three Universal Software Radio Peripherals (USRPs). Two of them send OFDM signals with the center frequency of 2.12 GHz and 0.96 MHz bandwidth, carrying different streams. The third USRP is connected to the right port of the prototype to receive the information from  $f_0 - \Delta f$ and  $f_0 + \Delta f$  frequencies. Table 1 depicts the measured BER in different scenarios. Initially, only one of the USRPs transmits the data, and the extracted stream from the corresponding harmonic component is compared with the sent stream by that USRP to calculate the BER. Then, both USRPs transmit their streams and the received data at  $f_0 - \Delta f$  is compared with the data sent by the USRP 1, while the received data at  $f_0 + \Delta f$  is compared with the data transmitted by the USRP 2. As observed, due to the good isolation between  $f_0 + \Delta f$ and  $f_0$  –  $\Delta f$  at  $\theta$  = 45°,  $\theta$  = 125°, low BERs are still achieved when both users send their own data at the same time. Fig. 6 indicates the constellation maps of the received signal from GNU Radio at two harmonic frequencies when both of the USRPs transmit their data. As can be seen, the QPSK constellation map is evident.

It is noted that, due to constraints in fabrication, our current prototype consists of just 9 cells, resulting in broader patterns as depicted in Fig. 4(a). This wide beamwidth hinders effective cross-beam isolation when dealing with more than two frequency components. As a result, our experimental measurements focus on a two-user scenario. However, if the antenna can be made to include a higher number of cells, leading to narrower beams, it would then be possible to efficiently extract data from several users.

Table 1. Measured BER

Sending User(s)	Extracted center frequency	Compared stream	BER
1	$f_0 - \Delta f \ (2.1163 \ \text{GHz})$	User 1	0.00194
2	$f_0 + \Delta f \ (2.1237 \ \text{GHz})$	User 2	0.00164
1 and 2	$f_0 - \Delta f \ (2.1163 \ \text{GHz})$	User 1	0.00213
1 and 2	$f_0 + \Delta f \ (2.1237 \ \text{GHz})$	User 2	0.00247



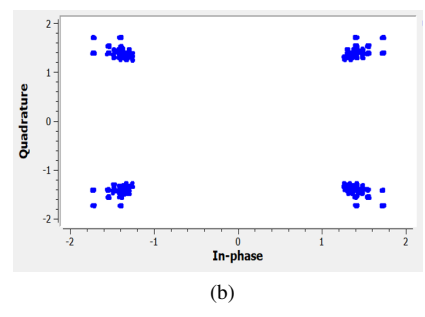


Fig. 6. Measured constellation map of the received signal through the USRP 3 at: (a)  $f_0 - \Delta f$  (2.1163 GHz); (b)  $f_0 + \Delta f$  (2.1237 GHz).

## IV. CONCLUSION

In this work, an ST-MTM antenna in reception mode is used to enable the mapping of incoming data from multiple users, each located in a different direction, to distinct harmonic frequency components generated within the antenna due to time modulation, thereby realizing beamspace MIMO. As a result, the transmitted information from each user can be retrieved from a specific harmonic frequency component. BER measurements are conducted in a scenario with two users sending data to the fabricated receiving antenna. These results confirm the spatial-spectral mapping capability of the proposed receiver, allowing for the retrieval of data from multiple users.

#### ACKNOWLEDGMENT

This work is supported by the National Science Foundation (NSF) under Grant ECCS-2229384, ECCS-2028823, and ECCS-2033433. Any opinions, findings, and conclusions or recommendations expressed in this material are those of the author(s) and do not necessarily reflect the views of the National Science Foundation.

#### REFERENCES

- [1] R. Maneiro-Catoira, J. Brégains, J. A. García-Naya, and L. Castedo, "Time modulated arrays: From their origin to their utilization in wireless communication systems," *Sensors*, vol. 17, no. 3, 2017. [Online]. Available: https://www.mdpi.com/1424-8220/17/3/590
- [2] J. Brady, N. Behdad, and A. M. Sayeed, "Beamspace mimo for millimeter-wave communications: System architecture, modeling, analysis, and measurements," *IEEE Transactions on Antennas and Propagation*, vol. 61, no. 7, pp. 3814–3827, 2013.
- [3] W. Kummer, A. Villeneuve, T. Fong, and F. Terrio, "Ultra-low sidelobes from time-modulated arrays," *IEEE transactions on antennas and* propagation, vol. 11, no. 6, pp. 633–639, 1963.
- [4] C. He, L. Wang, J. Chen, and R. Jin, "Time-modulated arrays: A four-dimensional antenna array controlled by switches," *Journal of Communications and Information Networks*, vol. 3, no. 1, pp. 1–14, 2018.
- [5] S. Vosoughitabar, A. Nooraiepour, W. U. Bajwa, N. Mandayam, and C.-T. M. Wu, "Metamaterial-enabled 2d directional modulation array transmitter for physical layer security in wireless communication links," in 2022 IEEE/MTT-S International Microwave Symposium-IMS 2022. IEEE, 2022, pp. 595–598.
- [6] A. Nooraiepour, S. Vosoughitabar, C.-T. M. Wu, W. U. Bajwa, and N. B. Mandayam, "Time-varying metamaterial-enabled directional modulation schemes for physical layer security in wireless communication links," J. Emerg. Technol. Comput. Syst., vol. 18, no. 4, oct 2022. [Online]. Available: https://doi.org/10.1145/3513088
- [7] S. Vosoughitabar, A. Nooraiepour, W. U. Bajwa, N. B. Mandayam, and C.-T. M. Wu, "Directional modulation retrodirective array-enabled physical layer secured transponder for protected wireless data acquisition," in 2023 IEEE/MTT-S International Microwave Symposium-IMS 2023. IEEE, 2023, pp. 1180–1183.
- [8] A. Nooraiepour, S. Vosoughitabar, C.-T. M. Wu, W. U. Bajwa, and N. B. Mandayam, "Programming wireless security through learning-aided spatiotemporal digital coding metamaterial antenna," Advanced Intelligent Systems, p. 2300341, 2023.
- [9] G. Bogdan, K. Godziszewski, and Y. Yashchyshyn, "Time-modulated antenna array with beam-steering for low-power wide-area network receivers," *IEEE Antennas and Wireless Propagation Letters*, vol. 19, no. 11, pp. 1876–1880, 2020.
- [10] T.-Y. Huang, B. Lin, N. S. Mannem, B. Abdelaziz, and H. Wang, "A time-modulated concurrent steerable multibeam mimo receiver array with spectral-spatial mapping using one beamformer and single-wire interface," *IEEE Journal of Solid-State Circuits*, vol. 58, no. 5, pp. 1228–1240, 2023.
- [11] C. Caloz and T. Itoh, *Electromagnetic metamaterials: transmission line theory and microwave applications*. John Wiley & Sons, 2005.
- [12] —, "Crlh metamaterial antennas, part ii: Leaky-wave and resonant antennas," in *Applications of Metamaterials*. CRC Press, 2017, pp. 16–1
- [13] S. Vosoughitabar and C.-T. M. Wu, "Programming nonreciprocity and harmonic beam steering via a digitally space-time-coded metamaterial antenna," *Scientific Reports*, vol. 13, no. 1, p. 7338, 2023.
- [14] S. Lim, C. Caloz, and T. Itoh, "Metamaterial-based electronically controlled transmission-line structure as a novel leaky-wave antenna with tunable radiation angle and beamwidth," *IEEE Transactions on Microwave Theory and Techniques*, vol. 53, no. 1, pp. 161–173, 2005.
- [15] B. Bloessl, M. Segata, C. Sommer, and F. Dressler, "Performance assessment of IEEE 802.11p with an open source SDR-based prototype," *IEEE Transactions on Mobile Computing*, vol. 17, no. 5, pp. 1162–1175, 2018.